 DOI: 10.1002/masy.200750614

Molecular Dynamics of Pectin Extension

Igor Neelov,[*1,2] *David Adolf,*[1] *Tom McLeish*[1]

Summary: A pectin 10mer under constant pulling speed and constant force was studied using the atomistic simulations. Molecular dynamics (MD) with the Amber99 and Amber-Glycam04 forcefields were performed. The main result of the present Amber-based MD simulations is that the two plateaux of the experimental force-extension dependence for pectin can be explained by transitions between three conformational states of pectin monomer ring (first from a chair ($^4C_1$) to boat conformation and second from boat to an inverted chair ($^1C_4$) conformation). A multi-state dynamical model of single biopolymer extension under external force was elaborated and applied to extension of polymers with three-state monomers relevant to pectin.

Keywords: extension; pectin; polysaccharides; single molecule AFM; three- states model

Introduction

Polysaccharides are fundamental components of cells and have many potential applications in the pharmaceutical industry and material science. Mechanical properties of polysaccharides are important because they constitute cell walls in plants and bacteria and take part in cell interactions and adhesion. They also serve as a simple model for studies into the mechanical properties of protein concatemers. Pectin is an important representative of polysacchrides with 1–4 linkages (i.e. connecting C_1 and C_4 carbon atoms on neighbouring sugar monomers). The mechanical extension of a pectin molecule in single molecule AFM experiments under constant pulling speed[1] and In the force-ramp regime[2] has been performed by Marszalek et al. A key finding was the existence of two plateaux in the force-extension dependence for pectin at forces near 400 and near 800pN. They suggested that the first plateau takes place due to conformational transition of monomer rings from chair to boat state and second plateau due to the transition from boat to inverted chair conformation. A review of these results was also published.

In the present paper, we study the extension of linear pectin molecule at constant pulling speed and constant force using an Amber-like forcefield.

Models and Methods of Molecular Simulation

Amber,[3] CHARMM[4] and some other forcefields (for example, MM3[5]) and their modifications (united atom Amber,[6] Amber-Homans,[7] Amber-Glycam,[8] Amber with GB/SA continuum model of water,[9] CHARMM-Parm22/SU01[10]) have been used for the simulations of monosaccharides.

A comparison of 20 different forcefields for monosaccharides was carried out recently.[11] The largest deviation from density functional results was observed for CHARMM22, Gromos, MM3* and some other forcefields. Surprisingly the best forcefield in this review was found to be the Amber-like forcefield (Amber94) which was not specially designed for carbohydrates.

In present work more recent versions of Amber forcefield (Amber99 and Amber-Glycam04) were used for molecular dynamics simulation of a linear pectin chain

[1] IRC in Polymer Science and Technology, University of Leeds, Leeds LS2 9JT, UK
E-mail: i.neelov@leeds.ac.uk
[2] Institute of Macromolecular Compounds, RAS, Bolshoi pr. 31, 199004, St.Petersburg, Russia

(polygalacturonic acid) consisting of 10 monomers *in vacuo* and in explicit water. In the first case two different values of the dielectric constant ($\varepsilon = 1$ and $\varepsilon = 80$) were used. The end-to-end vector of chain was initially oriented along X axis. The first chain end was fixed. In simulation with constant pulling speed the second end was restrained harmonically to another point which was moved with constant speed dx/dt (dx/dt = 0.01Å/ps) along the X axis. Several elasticity constants were used for this restraining from the interval 50-1000pN/nm to resemble the usual elasticity of cantilevers. The Verlet algorithm with a time step $\Delta t = 1$fs was used in all simulations. To achieve suitable local equilibration of pectin without explicit solvent molecules, the Andersen thermostat[12] was used.

Results and Discussion

Extension of Pectin 10mer at Constant Pulling Speed

The extension of a pectin 10mer was simulated at constant pulling speeds 0.01Å/ps.

Force-extension curves (i.e. force F acting on the pulled chain end in the direction of extension, as function of the extension) are presented in Figure 1 for 10mer without explicit water (Figure 1a for $\varepsilon = 1$ and Figure 1b for $\varepsilon = 78$) and in water (Figure 1c) for Amber99 forcefield. At small and high extensions in Figure 1a–1c the force depends linearly on extension in agreement with the experimental data. At the intermediate extensions (between 48 and 56Å) there are two clear plateau areas in accordance with experiment. But the values of plateau forces are higher than in experiment. For example for pectin *in vacuo* (Figure 1a and Figure 1b) the first plateau force is between 800pN and second plateau force is around 1200pN. For simulation in explicit water solvent (Figure 1c) the first plateau occurs at 800pN and second at 900pN. These values of plateau forces are greater than the experimental values (400 and 800 pN correspondingly) due to very high pulling speed in simulation in comparison with experiment.

Force-extension curves for AmberGlycam04 forcefield are presented in Figure 2 (Figure 2a for $\varepsilon = 1$ and Figure 2b for $\varepsilon = 78$ for 10mer *in vacuo*) and (Figure 1c for 10mer in water). The results for these forcefields are qualitatively similar to that for Amber 99 forcefield but there are some quantitative differences especially for position of both plateaux on force-extension curves. For pectin *in vacuo* (Figure 2a and Figure 2b) the first plateau force is between 600–800pN and second plateau force is around 900pN. For simulation in explicit water solvent (Figure 1c) first plateau occurs at 500–600pN and second at 800–900pN. The values of plateau forces for AmberGlycam04 forcefield (especially in water) are more close to experimental values (400 and 800 pN correspondingly) in

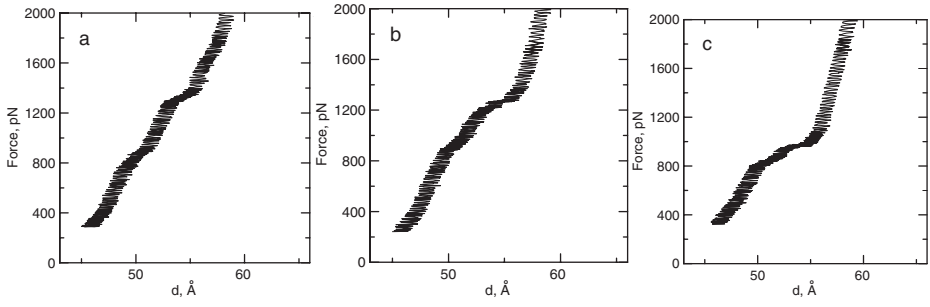

Figure 1.
Force-extension dependence for pectin 10mer extended at constant pulling speed 0.01Å/ps *in vacuo* at a) $\varepsilon = 1$, b) $\varepsilon = 80$ and c) in water. The data averaged over 200 points window. Amber99 forcefield.

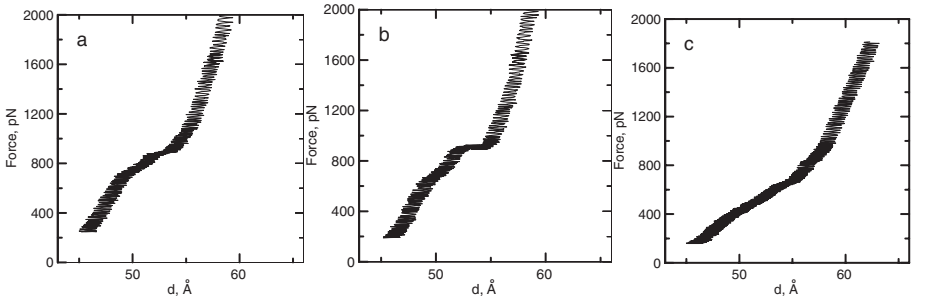

Figure 2.
Force-extension dependence for pectin 10mer extended at constant pulling speed 0.01Å/ps *in vacuo* at $\varepsilon = 1$, b) $\varepsilon = 80$ and c) in water. The data averaged over 200 points window. Amber-Glycam04 forcefield.

comparison with results for Amber99 forcefield.

To understand the molecular mechanisms of the pectin extension it is necessary to study the behaviour of monomers under extension. There are two ways of doing this. First, to study the extension behaviour of each monomer in the 10mer under extension. Second to perform an additional simulation of a single pectin monomer extension at constant pulling speed.

Figure 3 gives the dependence of length of each monomer in pectin 10mer for Amber99 forcefield as a function of time. It is easy to see that at short ($t < 500$ps) and at long ($t > 1300$ps) time (i.e until monomer length $d = 5.0$–5.1Å and after length $d = 5.7$–5.8Å only linear extension of the monomers occurs. In the interval of time $t = 500$–1300ps ($d = 5.1$–5.7Å), a step-like increase of monomer length occurs for all monomers. For some monomers it occurs as a single step-like transition and for others as two-stage transition through short-living intermediate conformation of the monomer with $d = 5.5$Å. At $\varepsilon = 1$ and in explicit water (Figure 3a and Figure 3c correspondingly) this intermediate state is more pronounced while at $\varepsilon = 80$ (Figure 3b) only tracks of this intermediate state exist.

Figure 4 gives the similar time dependences of length of monomers in pectin 10mer for AmberGlycam04 forcefield. It is easy to see that at short ($t < 500$ps) and at long ($t > 1300$ps) time (i.e until monomer length $d = 5.0$–5.1Å and after length $d = 5.7$–5.8Å only linear extension of the monomers occurs in agreement with results for Amber99 forcefield (Figure 3). In the interval of time $t = 500$–1300ps

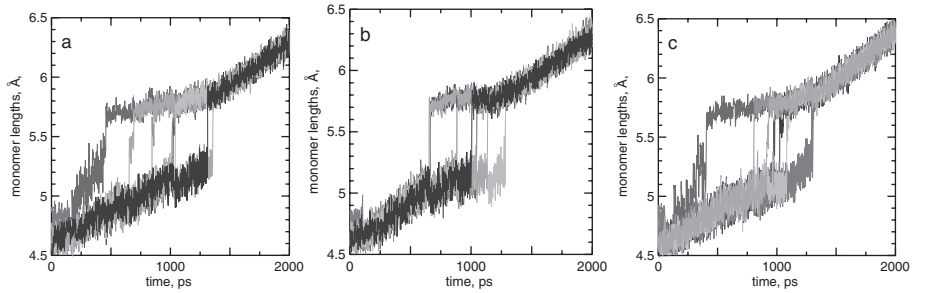

Figure 3.
The monomer lengths for monomers of pectin 10mer as function of time *in vacuo* a) $\varepsilon = 1$, b) $\varepsilon = 80$ and c) with explicit water. The data averaged over 200 points window. Amber99 forcefield.

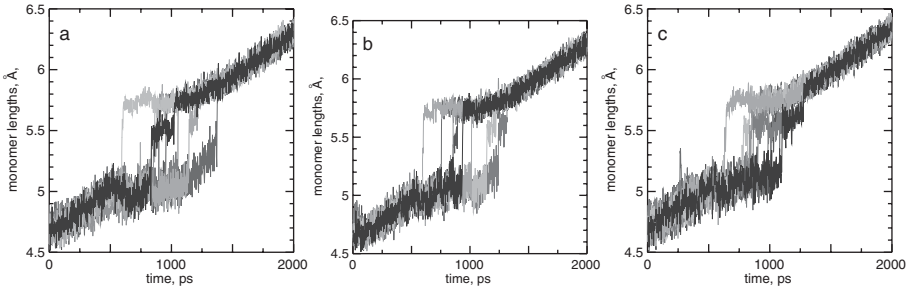

Figure 4.
The monomer lengths for monomers of pectin 10mer as function of time *in vacuo* at a) $\varepsilon = 1$, b) $\varepsilon = 80$ and c) in explicit water solvent. The data averaged over 200 points window. Amber-Glycam04 forcefield.

(d = 5.1– 5.7Å), a step-like increase of monomer length occurs for all monomers. Similarly to results for Amber99 forcefield some monomers undergo single step-like transition and some others - two-stage transition through intermediate conformation of monomer with d = 5.5Å. Again as for Amber99 forcefield this intermediate state is more pronounced at $\varepsilon = 1$ and in explicit water (Figure 4a and Figure 4c correspondingly). In all cases (Figure 4a–Figure 4c) the intermediate state is more pronounced for AmberGlycam04 than for Amber99 forcefield.

Extension of Pectin 10mer by Constant Force

Similar time dependences of length of monomers in pectin 10mer were obtained for at constant force applied to chain ends. At small forces all monomer lengths fluctuate around the same value equal 4.7–4.8Å. At high forces all monomers are in another (long) state with monomer length fluctuating around 5.7 Å. At intermediate forces (400–1400pN) the picture is more complicated and third (intermediate) state with intermediate monomer length occurs. For example at force F = 1000pN (Figure 3) there are monomers in different states with three different average lengths. For Amber99 (Figure 3a) these values are 4.7, 5.2 and 5.7Å while for AmberGlycam04 *in vacuo* and in water (Figure 3b and Figure 3c correspondingly) they are 4.7, 5.5 and 5.7Å. Increase of force leads to increase of population of intermediate and long states at intermediate forces and to increase of population of long states at high forces.

Theory of Multi-state Dynamical Model

Mechanical extension of biopolymers (protein concatemers, DNA, RNA, polysaccharides) in single molecule atomic force

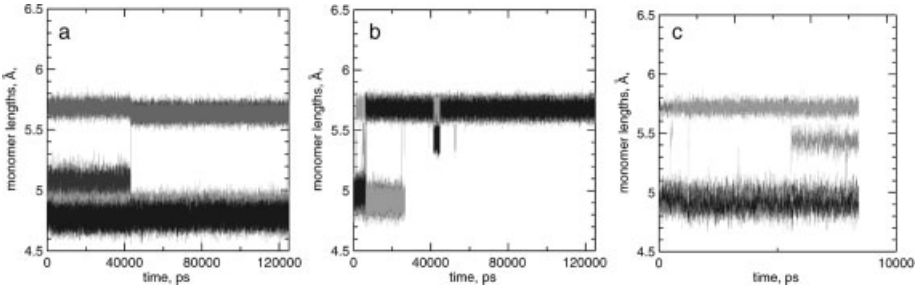

Figure 5.
The monomer length as function of time at constant force F = 1000pN in vacuo for a) $\varepsilon = 1$ and Amber99 and b) $\varepsilon = 1$ and Amber-Glycam04 forcefields and c) in water for Amber-Glycam04 forcefield.

microscopy (AFM) experiments is a well established technique for determination of mechanical properties and study of pathways of forced unfolding and refolding. Polysaccharide molecules were frequently used as simple test objects in AFM experiments and simulation (Rief et al.,[13] Marszalec et al.,[14] Lee et al.,[15]) and for elaboration of theoretical models. A discrete two-state model is usually used for a theoretical description of an extension of protein concatemers, polysaccharides and other biopolymers in AFM. In this model each element can exist in two states: folded and unfolded. But it is well known that some proteins and polysaccharides can have one or more additional intermediate states. In present paper we elaborate a discrete multistate theoretical model and obtain the results for particular case of three-state theoretical model.

Model and Method of Calculations

Our theoretical consideration of biopolymer extension by mechanical force applied to its end is based on a multi-state population model. We study populations of states under the simultaneous action of a large constant and a small periodical force $F = F_0 + f_0 \; cos \; \omega \; t$ where t is time, ω is frequency of oscillations and magnitude of small force f_0 is significantly smaller than magnitude of constant force F_0. The population at any time moment t is defined by an equation

$$d\vec{p}(t)/dt = \Lambda\vec{p}(t) \tag{1}$$

where p is a multidimensional population vector $p = (p_1, p_2, \ldots, p_N)$, t is a time and Λ is a matrix which contains rates of transition λ_{ij} between states i and j (where i and j are from *1* to N and N is a number of states).

In the absence of force the rate of conformational transition $\lambda_{i,j}$ depends on height of free energy barrier $\Delta G_{i,j}$ or transition from i to j state. An application of force F changes the barrier in accordance with the phenomenological Bell equation

$$\lambda_{i,j} = \lambda_0 \exp[-\beta(\Delta G_{i,j} + F\Delta x_{i,j})] \tag{2}$$

where $\lambda_{i,j}$ are rates of transition between *i-th* and *j-th* states, $\beta = 1/k_B\,T$ is the reciprocal thermal energy, $\Delta G_{i,j}$ is the height of free energy barrier in the absence of force, F is the force applied to the system and $\Delta x_{i,j}$ is the effective difference between coordinate of *i-th* minimum and coordinate of barrier between *i-th* and *j-th* states.

For normalized values of populations (i.e. for probabilities of different states) there is an additional condition $p_1 + p_2 + \ldots + p_N = 1$. Taking it into account we can go from N component vector p to N-1 component vector q which will contain only linearly independent components.

$$\frac{d\vec{q}}{dt} = -J\vec{q} + \vec{s} \tag{3}$$

If the fluctuating component of external force is essentially smaller than constant force (i.e. if $F_0 \gg f_0$) we can represent all components of this equation as sum of equilibrium values and small variations

$$\vec{q} = \vec{q}_0 + \delta\vec{q} \quad ; \quad \vec{s} = \vec{s}_0 + \delta\vec{s} \quad \text{and} \quad J = J_0 + \delta J \tag{4}$$

Rates of transition $\lambda_{i,j}$ between i and j states also can be presented as a sum of equilibrium rate and linear variation:

$$\lambda_{i,j} \approx \lambda^0_{i,i+1}(1 + f_0 \cos\omega t \Delta x_{i,i+1}) = \lambda^0_{i,i+1} + \delta\lambda_{i,i+1} \tag{5}$$

In this case Equation (3) can be rewritten in the form

$$\frac{d(\vec{q}_0 + \delta\vec{q})}{dt} = -(J_0 + \delta J)(\vec{q}_0 + \delta\vec{q}) + \vec{s}_0 + \delta\vec{s} \tag{6}$$

An equilibrium solution can be obtained from

$$\frac{d\vec{q}_0}{dt} = 0 = -J_0\vec{q}_0 + \vec{s}_0 \tag{7}$$

in the form

$$\vec{q}_0 = J_0^{-1}\vec{s}_0 \tag{8}$$

The equation for δq can be obtained by subtracting Equation (7) from

Equation (6):

$$\frac{d\delta\vec{q}}{dt} = -J_0\delta\vec{q} - \delta J\vec{q}_0 + \delta\vec{s} \tag{9}$$

which can be presented in the form

$$\frac{d\delta\vec{q}}{dt} = -J_0\delta\vec{q} + \vec{g}f_0\cos wt \tag{10}$$

where

$$\vec{g} = -\delta J\vec{q}_0 + \delta\vec{s} \tag{11}$$

The general solution for δq in this case will have a form

$$\delta\vec{q} = [w^2 I + J_0^2]^{-1} \times [J_0\cos wt + I\ \sin wt] + \vec{g} \tag{12}$$

where I is a unit matrix and the value of g in linear approximation depend only on equilibrium rates of transition $\lambda i,j0$ and distances $\Delta x_{i,j}$ between the energy minima and the barriers.

We apply this algorithm to the case of three-state model with equilibrium matrix of transition rates Λ_0

$$\Lambda_0 = \begin{bmatrix} -\lambda_{12}^0 & \lambda_{21}^0 & 0 \\ \lambda_{12}^0 & -\lambda_{12}^0 - \lambda_{23}^0 & \lambda_{32}^0 \\ 0 & \lambda_{23}^0 & -\lambda_{32}^0 \end{bmatrix} \tag{13}$$

It means that we study system with three states and ''one dimensional'' mechanism of transitions between them when there are transitions between 1st and 2nd states as well as between 2nd and 3rd states but direct transitions between 1st and 3rd states are absent. Due to a condition $p_1 + p_2 + p_3 = 1$ we have only two independent variables. If we choose as independent variables $q_1 = p_1$ and $q_2 = p_3$ then matrix J_0 (from Equation (4)) have form

$$J_0 = \begin{bmatrix} \lambda_{12}^0 + \lambda_{23}^0 & \lambda_{21}^0 \\ \lambda_{23}^0 & \lambda_{12}^0 + \lambda_{23}^0 \end{bmatrix} \tag{14}$$

Equilibrium population can be obtained from Equation (8) and Equation (14) in form:

$$\begin{aligned} P_1^0 &= \frac{\lambda_{21}^0\lambda_{32}^0}{\lambda_{12}^0\lambda_{23}^0 + \lambda_{12}^0\lambda_{32}^0 + \lambda_{21}^0\lambda_{32}^0} \\ P_2^0 &= \frac{\lambda_{12}^0\lambda_{32}^0}{\lambda_{12}^0\lambda_{23}^0 + \lambda_{12}^0\lambda_{32}^0 + \lambda_{21}^0\lambda_{32}^0} \\ P_3^0 &= \frac{\lambda_{12}^0\lambda_{23}^0}{\lambda_{12}^0\lambda_{23}^0 + \lambda_{12}^0\lambda_{32}^0 + \lambda_{21}^0\lambda_{32}^0} \end{aligned} \tag{15}$$

To get the population at any time we need to substitute equilibrium transition rates from Equation (15) in Equation (12) and result in Equation (4). The final result for populations is rather complicated. However, we are interested not in the population itself but how the length of chain changes with force and how the value of elasticity constant change with force. The result for the length of the chain is

$$L(t) = L_0 + f_0\left(\frac{(\cos\omega t + \omega\tau_1\sin\omega t)}{K_1(1+\omega^2\tau_1^2)} + \frac{(\cos\omega t + \omega\tau_2\sin\omega t)}{K_2(1+\omega^2\tau_2^2)}\right) \tag{16}$$

The length at zero frequency $\omega = 0$ is

$$L = L_0 + f_0\left(\frac{1}{K_1} + \frac{1}{K_2}\right) \tag{17}$$

where L_o is the length without force and K_1 and K_2 are rather complicated functions.

It is easy to see that the total elasticity constant at zero frequency can be written as

$$K^{-1} = K_1^{-1} + K_2^{-1} \tag{18}$$

and a final equation for it has a simple form

$$K = \frac{k_B T}{\left(p_1^0 p_2^0 x_2^2 + p_2^0 p_3^0 (x_3 - x_2)^2 + p_1^0 p_3^0 x_3^2\right)} \tag{19}$$

where $p^o{}_1$, $p^o{}_2$, $p^o{}_3$ are equilibrium populations of first, second and third states and x_2 and x_3 are distances between first and second or between first and third states (i.e. between positions of the first minimum and the second or the third minima of energy) correspondingly.

We calculated the length L using Equation (17), Equation (18) and Equation (19) and as function of force in Figure 6 for two different cases: when distances

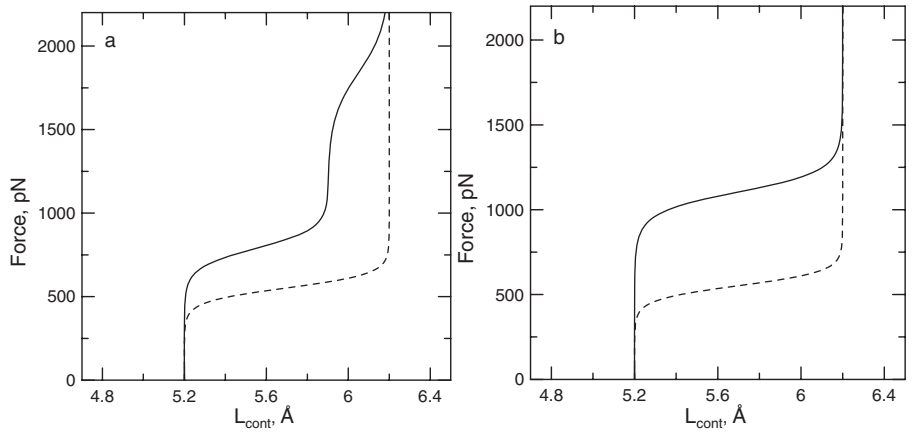

Figure 6.
Force-extension curve for 3state model: force vs normalized contour length for: a) $x_2 = 0.7x_3$ and b) $E_2 = 8$kcal/mol, $E_3 = 16$ kcal/mol and $x_2 = 0.5x_3$. (solid lines are for $E_2 = 8$kcal/mol and $E_3 = 16$ kcal/mol and dashed line for $E_1 = E_2 = 8$kcal/mol). Value $d_1 = 5.2$ Å, $d_2 = 5.9$ Å and $d_3 = 6.2$ Å corresponds to short, intermediate and long monomer length in dextran obtained by us in previous paper using simulation with full atomic details.

$x_2 = 0.5x_3$ and when $x_2 = 0.7x_3$. For solid lines the energies of 1st, 2nd and 3rd states were *E = 0, 8 and 16 kcal/mol* correspondingly (for dashed lines *E = 0, 8* and *8kcal/mol*). We obtained that when the second state is closer to the third one ($x_2 = 0.7x_3$) and energy of the third state is higher than energy of second state (Figure 6A, solid line) the force-extension dependence has two plateaux. A first plateau is at 800-100pN and a second is at forces near 1600pN. But at the same $x_2 = 0.7x_3$ and $E_2 = E_3 = 8kcal/mol$ (Figure 6A, dashed line) there is only one plateau at forces near 500pN. Similarly, when the second state is in the middle position between the first and the third state ($x_2 = 0.5x_3$, Figure 6B) the force-extension dependence has only one plateau region at forces near 800-1000pN. The dependence with only one plateau is similar to that obtained earlier for a two-state model[16] while the second plateau appears only for three-state systems. Thus we found that the force-extension dependence for three-state systems can look both like two-state or like three-state depending on parameters (energies and distances) of states.

Similar results were obtained by us using full atomic simulation of dextran 10mer[17] (as well as simulation of pectin 10mer in this paper). In the dextran paper we have shown that during the extension of dextran the monomers can exist in three different states (short, intermediate and long). A simulation with first forcefield gives the force-extension curve with two plateaux at the same forces (800-1000pN and near 1600N) as our three-state discrete population model with $x_2 = 0.7x_3$ and $E_3 > E_2$ (solid curve, Figure 1A). However, a simulation with second forcefield gives only one plateau for the same system similarly to our results for theoretical model with $x_2 = 0.7x_3$ and $E_3 = E_2$ (Figure 6A dashed line) or with $E_3 > E_2$ and $x_2 = 0.5x_3$ (Figure 6B).

Total inverse elasticity $1/K_{TOT}$ (compliance) of biopolymer chain under extension can be calculated as sum of inverse elasticities of all processes. For chain consisting of two-state monomers the result was obtained by McLeish and Khatri.[17] It takes into account elasticity of freely-joint chain K_{FJK}, important at small forces, elasticity around each of the minima K_{01} and K_{02} (chair and boat states of glucopyranose ring in the case of dextran) and elasticity due to transition from first to second conformational state of monomer

K_1 (i.e. from chair to boat state for dextran):

$$\frac{1}{K_{tot}} = \left(\frac{1}{K_{FJK}} + \frac{p_1^0}{K_{01}} + \frac{p_2^0}{K_{02}} + \frac{1}{K_1}\right) \quad (20)$$

We extended this approach to the case of chain consisting of three-state monomers and added elasticity around third minima K_{03} (elasticity of inverted chair state in the case of pectin) and elasticity due to transitions from second to third state K_2 (i.e. from boat to inverted chair for pectin):

$$\frac{1}{K_{tot}} = \left(\frac{1}{K_{FJK}} + \frac{p_1^0}{K_{01}} + \frac{p_2^0}{K_{02}} + \frac{p_3^0}{K_{03}} + \frac{1}{K_1} + \frac{1}{K_2}\right) \quad (21)$$

Total elasticity coefficient as function of force for three-state model were calculated and presented in Figure 7 for the case when energies of first and third state $E_1 = 0$ kcal/mol and $E_3 = 16$ kcal/mol and distance between first and third minimum $x_2 + x_3 = 1$Å.

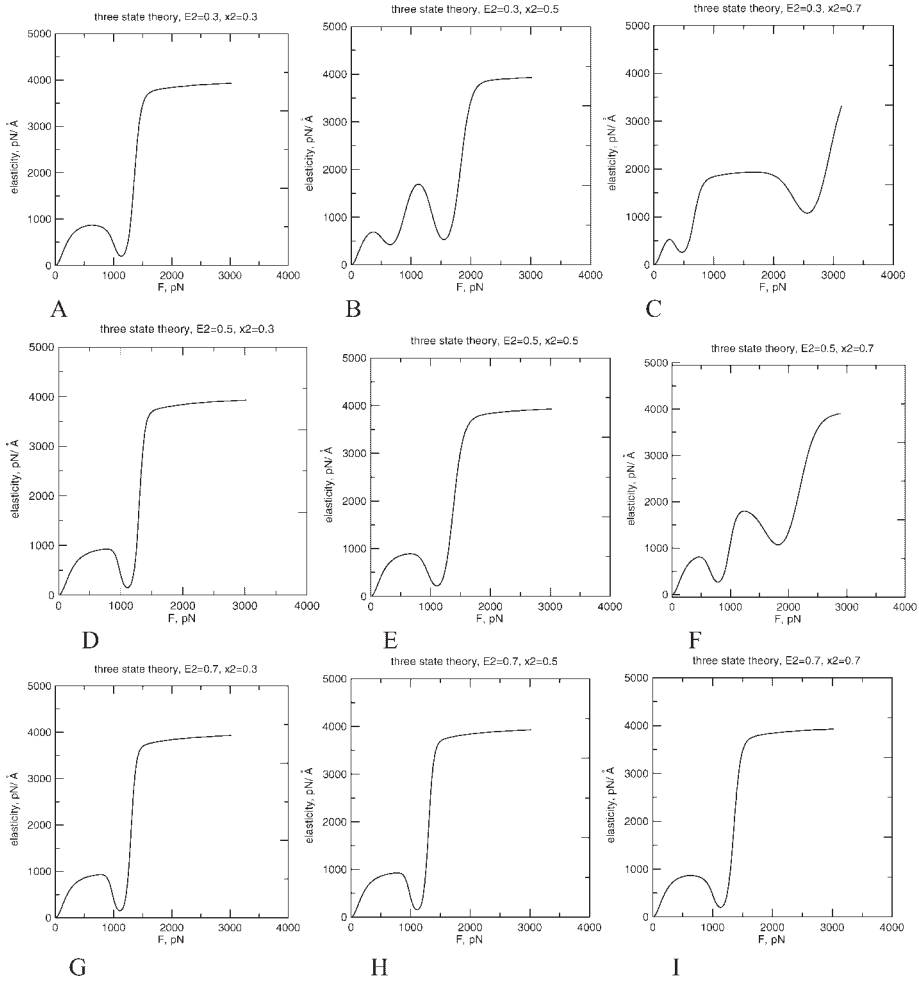

Figure 7.
Total elasticity coefficient as function of force for three-state model with the same energy difference between first and third states ($E_3 = 16$ kcal/mol) and distance between first and third state ($x_3 = 1$Å) and different energy (E_2) and position (x_2) of second state relatively first state. Distance, x_2, increases from left to right: A), D), G) $x_2 = 0.3x_3$; B), E), H) $x_2 = 0.5x_3$; C), F), I) $x_2 = 0.7x_3$ and energy, E_2, changes increases up to down A, B, C) $E_2 = 0.3E_3$; D, E, F) $E_2 = 0.5E_3$; and G, H, I) $E_2 = 0.7E_3$.

Elasticity at different energies of second state E_2 and positions of second state x_2 are presented in Figure 7A–Figure 7I. Distance x_2 increases from left to right (for example, from Figure 7A to Figure 7C in first row) and energies from up to down (from Figure 7A to Figure 7G in first column).

It is easy to see that at small values of distances $x_2 = 0.3x_3$ between the first and second minima or at high energy of the second state $E_2 = 0.7E_3$ the elasticity always has only one minimum on force dependence, typical for two state model. It occurs because the population of the third state increases with force quicker than population of second state. At other values of $x_2 = 0.5x_3$ or $E_2 = 0.5E_3$ the situation depends on both parameters and a typical three-state picture is manifest, for example at Figure 7B, Figure 7C and Figure 7F.

Conclusion

The pectin extension at constant pulling speed and by constant force were simulated using model with full atomic details and Amber99 and Amber-Glycam04 forcefield. The main result of the present Amber-based simulation is that there are two plateaux on the force-extension dependence. These two plateaux can be explained by a transition of the monomer rings from the extended chair ($^4C_1$) d = 4.7 Å to the extended boat (intermediate state) d = 5.2–5.5 Å and to extended inverted chair ($^1C_4$) d = 5.7Å conformation. The lengths of pectin monomer in chair, boat and inverted chair conformations are in agreement with lengths (d = 4.5, 4.9-5.0 and 5.4–5.5 Å) obtained in *ab initio* calculations cited by Marszalek et al.,[1–3] taking into account that monomers in AFM experiments are slightly extended in each conformation state in comparison with corresponding unperturbed states in *ab initio* calculations.

A multi-state dynamical model of single biopolymer extension under external force was elaborated and applied to extension of polymers with three-state monomers relevant to pectin polymer or concatemers of globular proteins with intermediate states. It was shown that elasticity of three-state systems can looks similar to elasticity of two-state systems in a broad parameter range describing the structure of the intermediate state. This makes difficult an experimental separation of two- and three-state systems from results of single molecule AFM experiments. This work was supported by EPSRC, grants GR/S67388/01 and EP/C528336/1. I.N. is thankful for partial support to INTAS (grant ref. Nr 05-1000004-7747).

[1] P. E. Marszalek, Y.-P. Pang, H. Li, J. E. Yazal, A. F. Oberhauser, J. M. Fernandez, *PNAS* **1999**, *96*, 7894–7898.
[2] P. E. Marszalek, H. Li, A. F. Oberhauser, J. M. Fernandez, *PNAS* **2002**, *99*, 4278–4283.
[3] S. J. Weiner, P. A. Kollman, D. T. Nguen, D. A. Case, *J. Comput. Chem.* **1986**, *7*, 230.
[4] MacKerell, et al. CHARMM22 *J.Phys.Chem.B* **1998**, *102*, 3586.
[5] M. K. Dowd, A. D. French, P. J. Reilly, *Carbohydrate Research*, **1994**, *264*, 1.
[6] H. Senderovitz, C. Parish, W. C. Still, *J. Am. Chem. Soc.* **1996**, *118*, **2078**.
[7] S.W. Homans, *Biochemistry* **1990**, *29*, 9110.
[8] R. J. Woods, et al. *J.Phys.Chem.* **1995**, *99*, 3832.
[9] H. Senderovitz, W. C. Still, *J. Org. Chem* **1997**, *62*, 1427.
[10] R. Eklund, G. Widmalm, *Carbohydrate Research* **2003**, *338*, 393.
[11] L. Hemmingsen, et al. *Carbohydrate Research* **2004**, *339*, 937.
[12] H. C. Andersen, *J.Chem.Phys.* **1980**, *72*, N4, 2384–2393.
[13] M. Rief, F. Oesterhelt, B. Heymann, H. E. Gaub, *Science* 1997, *275*, 1295–1297.
[14] P. E. Marszalek, A. F. Oberhauser, Y. P. Pang, J. M. Fernandez, *Nature* **1998**, *396*, 661–664.
[15] G. Lee, W. Nowak, J. Jaroniec, Q. M. Zhang, P. E. Marszalek, **2004**.
[16] M. Kawakami, K. Byrne, B. Khatri, T. C. B. McLeish, S. E. Radford, D. A. Smith, *Langmuir* **2004**, *20*, 9299; *Langmuir* **2005**, *21*, 4765.
[17] I. Neelov, D. Adolf, E. Paci, T. McLeish, *Biophys. J* **2006**, *91*, 3579–3588.

